

Soft Clustering Anchors for Self-Supervised Speech Representation Learning in Joint Embedding Prediction Architectures

Georgios Ioannides^{1,3,7} Adrian Kieback^{3,*} Judah Goldfeder^{4,*} Linsey Pang⁵

Aman Chadha^{3,6} Aaron Elkins³ Yann LeCun² Ravid Shwartz-Ziv²

¹Carnegie Mellon University ²New York University ³James Silberrad Brown Center for AI

⁴Columbia University ⁵Northeastern University ⁶Stanford University ⁷Amazon GenAI[†]

*Equal contribution Correspondence: gioannid@alumni.cmu.edu

Abstract

Joint Embedding Predictive Architectures (JEPA) offer a promising approach to self-supervised speech representation learning, but suffer from representation collapse without explicit grounding. We propose GMM-Anchored JEPA, which fits a Gaussian Mixture Model once on log-mel spectrograms and uses its frozen soft posteriors as auxiliary targets throughout training. A decaying supervision schedule allows GMM regularization to dominate early training before gradually yielding to the JEPA objective. Unlike HuBERT and WavLM, which require iterative re-clustering, our approach clusters input features once with soft rather than hard assignments. On ~ 50 k hours of speech, GMM anchoring improves ASR (28.68% vs. 33.22% WER), emotion recognition (67.76% vs. 65.46%), and slot filling (64.7% vs. 59.1% F1) compared to a WavLM-style baseline with matched compute. Cluster analysis shows GMM-anchored representations achieve up to 98% entropy compared to 31% for WavLM-style, indicating substantially more uniform cluster utilization. Code is made available*.

Keywords: Self-supervised learning, speech representation, JEPA, Gaussian mixture models

1 Introduction

Self-supervised learning has become the dominant paradigm for speech representation learning [3, 16, 9]. Joint Embedding Predictive Architectures (JEPA) [21, 1] offer a promising direction by predicting latent representations rather than reconstructing inputs or contrasting samples, avoiding the need for iterative re-clustering that dominates current speech SSL methods. However, when applied to speech, we find that JEPA suffers from severe representation collapse: without precautions, JEPAs map

inputs to degenerate representations [13, 1]. In our experiments, unanchored JEPA produces near-random predictions on downstream ASR, indicating that the encoder discards phonetic distinctions entirely. Our goal is not to achieve state-of-the-art absolute performance, but to demonstrate that frozen acoustic anchors can stabilize JEPA training for speech, eliminating the need for iterative re-clustering while maintaining competitive downstream performance.

Existing solutions to representation collapse in speech SSL rely on iterative offline clustering. HuBERT [16] and WavLM [9] fit k-means on intermediate representations, retrain the model with new targets, and repeat. This costly pipeline multiplies training compute. These methods also use hard cluster assignments, discarding uncertainty at acoustic boundaries.

We propose to anchor JEPA training with a frozen Gaussian Mixture Model fitted once on log-mel spectrograms (Figure 1). Because the GMM is frozen, it provides stable acoustic targets that cannot co-adapt with the encoder. An auxiliary Kullback-Leibler (KL) divergence loss matches a cluster head’s output to the GMM’s soft posteriors, with weight decaying from $\lambda = 1.0$ to $\lambda = 0.01$ over training so that cluster supervision dominates early while the JEPA objective gradually takes over. Unlike HuBERT and WavLM, which require iterative re-clustering of intermediate representations, our GMM is fitted once on input features. And unlike hard k-means assignments, GMM posteriors preserve uncertainty at cluster boundaries, which we hypothesize provides richer supervision signal.

On approximately 50k hours of speech, GMM-anchored JEPA reduces WER by 14% relative on LibriSpeech [27] compared to a WavLM-style baseline with matched compute, while also improving emotion recognition and slot filling. Cluster analysis reveals that GMM-anchored representations achieve up to 98% entropy versus 31% for WavLM-style, indicating substantially more uniform cluster utilization.

[†]Work does not relate to position at Amazon.

*<https://github.com/gioannides/clustering-anchored-jepa>

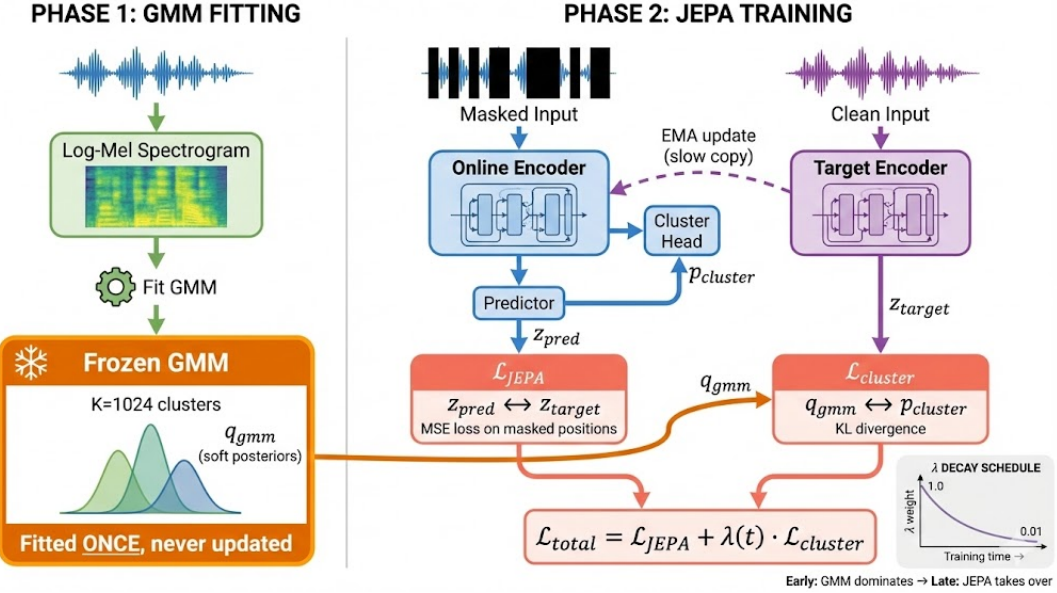


Figure 1: **GMM-Anchored JEPA: one-time clustering replaces iterative re-training.** **Phase 1:** A GMM is fitted once on log-mel features. **Phase 2:** The encoder trains with two objectives: predicting masked EMA teacher latents (JEPA loss) and matching frozen GMM posteriors (cluster loss). $\lambda(t)$ decays from 1.0 to 0.01.

Contributions.

- We identify representation collapse in JEPA-based speech SSL and propose *frozen GMM anchoring* with a decaying supervision schedule, replacing iterative re-clustering with one-time soft clustering of input features.
- We demonstrate that residual GMM supervision ($\lambda = 0.01$) provides ongoing regularization throughout training: removing it causes representations to collapse even after initial grounding, showing that GMM anchoring is not merely initialization but continuous stabilization.
- We show that GMM anchoring generalizes across encoder architectures (Conformer and Transformer), improving downstream performance on ASR, emotion recognition, and slot filling while achieving up to 98% cluster entropy compared to 31% for WavLM-style baselines.

2 Related Work

Self-Supervised Speech Learning. Contrastive methods (CPC [30], wav2vec 2.0 [3]) distinguish positive from negative samples, but require negative sampling strategies and codebook diversity losses to avoid collapse. Masked prediction methods (HuBERT [16], WavLM [9]) use offline k-means clustering for discrete targets, iteratively re-clustering intermediate layers, which multiplies training compute and requires careful scheduling. BEST-RQ [10] avoids re-clustering by using a frozen random-projection

quantizer, but provides random rather than acoustically informed targets. JEPA [21, 1] predicts latent representations directly without reconstruction or negatives, but suffers from representation collapse in speech without external grounding.

Self-Distillation and Collapse. BYOL [15] and DINO [8] showed that self-distillation with an EMA teacher can learn without negatives, using centering, sharpening, or asymmetric architectures to prevent collapse. data2vec [2] applies this to speech, predicting averaged teacher representations across layers. However, representation collapse remains a challenge in self-supervised learning [19], particularly for speech where the EMA teacher provides no spectral grounding. The issue is that EMA-based teachers in speech SSL provide only temporal smoothing without acoustic anchoring: the teacher’s representations drift alongside the student, offering no stable reference to ground phonetic distinctions. Our work addresses this by anchoring JEPA with frozen GMM supervision that cannot co-adapt with the encoder.

Clustering Supervision. HuBERT and WavLM use hard k-means assignments that discard uncertainty at cluster boundaries [23, 4]. When a frame lies between two phonetic categories, hard assignment forces an arbitrary choice, losing information about the acoustic ambiguity. GMMs have long been used in speech processing [5], where soft posteriors naturally model the gradual transitions between phonemes. Like BEST-RQ, we use a frozen clustering model to avoid iterative re-training, but unlike BEST-RQ’s random projections, our GMM provides acous-

tically meaningful soft posteriors fitted to the input feature space. The frozen GMM serves as an external anchor that grounds representations in spectral structure while the decaying supervision schedule allows the JEPA objective to refine higher-level abstractions.

3 Method

3.1 Framework Overview

Our framework has two phases. In the first, a Gaussian Mixture Model is fitted once on log-mel spectrograms, producing soft posterior targets over K clusters. In the second, a student encoder f_ϕ trains jointly with two objectives: (1) predicting masked latent representations from an EMA teacher $f_{\phi'}$, and (2) matching a cluster head’s output to the frozen GMM posteriors. The GMM is never updated during training.

3.2 Phase 1: GMM Fitting

A K -component diagonal-covariance GMM is fitted on log-mel features $M = \log(\text{MelSpec}(\mathbf{x}) + \epsilon)$. We use log-mel spectrograms rather than raw waveforms or learned features because they provide a stable, low-dimensional acoustic representation that does not change during training. Diagonal covariance keeps fitting tractable on large corpora while still capturing per-frequency variance. The GMM produces soft posterior assignments:

$$q_k(\mathbf{m}) = \frac{\pi_k \mathcal{N}(\mathbf{m}; \boldsymbol{\mu}_k, \sigma_k^2)}{\sum_j \pi_j \mathcal{N}(\mathbf{m}; \boldsymbol{\mu}_j, \sigma_j^2)}. \quad (1)$$

Unlike hard k -means labels, these posteriors assign nonzero probability to multiple clusters, so frames near a boundary are not forced into a single partition.

3.3 Phase 2: Joint Training

JEPA Loss. A predictor h_ψ predicts EMA teacher latents at masked positions:

$$\mathcal{L}_{\text{JEPA}} = \frac{1}{|\mathcal{M}|} \sum_{t \in \mathcal{M}} \|h_\psi(\tilde{z}_{\text{student}})_t - z_{\text{teacher},t}\|^2. \quad (2)$$

Cluster Loss. A cluster head maps encoder outputs to K logits, trained to match GMM posteriors:

$$\mathcal{L}_{\text{cluster}} = \frac{1}{|\mathcal{M}|} \sum_{t \in \mathcal{M}} \text{KL}(q_{\text{gmm},t} \| p_{\text{cluster},t}). \quad (3)$$

Total Loss with Decay.

$$\mathcal{L}_{\text{total}} = \mathcal{L}_{\text{JEPA}} + \lambda(t) \cdot \mathcal{L}_{\text{cluster}}, \quad (4)$$

where $\lambda(t)$ decays linearly from 1.0 to 0.01. Early training is thus dominated by GMM supervision, grounding

representations in acoustic structure. As λ decays, the JEPA objective takes over while residual anchoring prevents drift. We use KL divergence because both q_{gmm} and p_{cluster} are distributions over K clusters, and KL penalizes mismatched modes more heavily than L2. The residual weight $\lambda_{\text{end}} = 0.01$ is retained rather than reduced to zero: as shown in Section 5, removing the anchor entirely causes representation collapse.

3.4 Denoising Augmentation

Denoising augmentation with energy-based mixing is applied to improve the robustness of the student encoder (i.e. the Online Encoder being trained via gradient based optimization). The target encoder (i.e. the network which is a delayed copy of the Online Encoder) sees clean audio while the online encoder sees augmented audio, encouraging denoising in learned representations.

Noise Addition. Given clean waveform $\mathbf{x}_{\text{clean}}$ and noise \mathbf{n} , the target mixing Signal-to-Noise Ratio (SNR) is set at:

$$\mathbf{x}_{\text{aug}} = \mathbf{x}_{\text{clean}} + \alpha \cdot \mathbf{n}, \quad \alpha = \sqrt{\frac{E_{\text{clean}}}{10^{\text{SNR}/10} \cdot E_{\text{noise}}}}, \quad (5)$$

where $E = \frac{1}{N} \sum_i x_i^2$ denotes energy and SNR is sampled from $[-5, 20]$ dB with probability 0.25.

Utterance Mixing. A segment from another utterance is mixed with energy-based weighting:

$$\mathbf{x}_{\text{mix}}[t_1 : t_2] = \mathbf{x}_1[t_1 : t_2] + \beta \cdot \mathbf{x}_2[s_1 : s_2], \quad (6)$$

where $\beta = \sqrt{E_1 \cdot 10^{\rho/10} / E_2}$ with $\rho \sim [-5, 5]$ dB. Mixing probability is 0.25 with max 50% overlap.

3.5 Training Algorithm

The complete training procedure is summarized in Algorithm 1. Block masking samples spans of 10-25 frames until 40-65% masked. After training, only f_ϕ is retained.

3.6 Architecture

The encoder uses strided convolutions followed by a Conformer stack. Total stride $[8 \times 8 \times 5] = 320$ yields 20ms frames at 16kHz. Each strided block applies convolution, Snake-Beta activation [32], residual dilated convolutions, and density-adaptive attention [17]. The Conformer stack uses 4 layers with gated relative position bias and layer aggregation via cross-attention.

Masking Strategy. Block-wise temporal masking samples contiguous spans of length 10–25 frames until 40–65% of positions are masked. A learned mask token $\mathbf{t}_{\text{mask}} \in \mathbb{R}^C$ replaces masked positions.

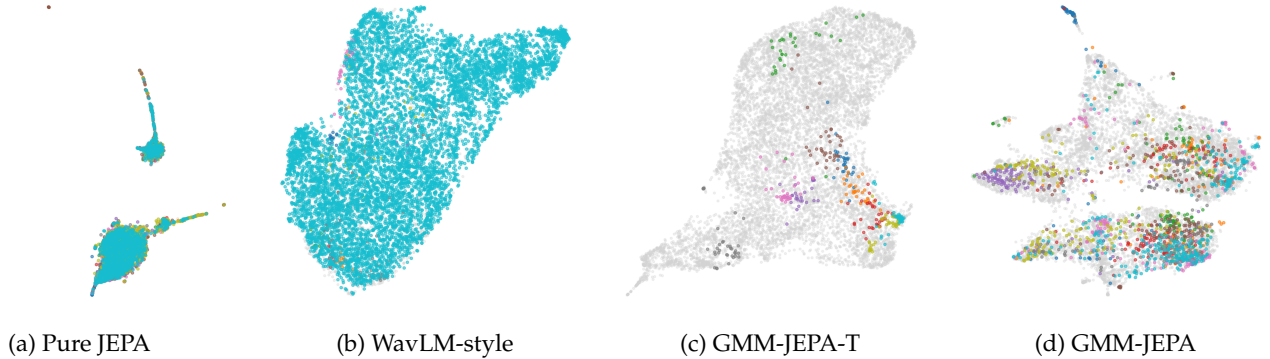


Figure 2: **GMM-JEPA learns well-separated clusters; baselines collapse or overlap.** UMAP of frame-level embeddings colored by predicted cluster. (a) Pure JEPA collapses. (b) WavLM-style overlaps. (c,d) GMM-JEPA variants form distinct regions.

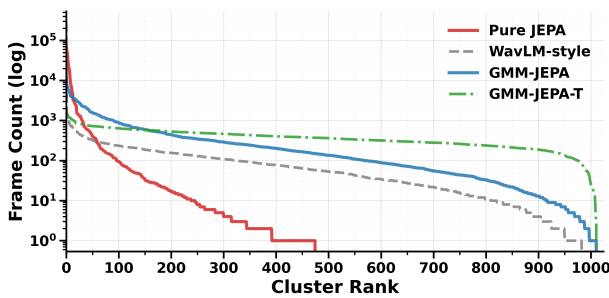


Figure 3: **GMM-JEPA uses all clusters uniformly; baselines collapse to few.** Frame counts per cluster (log scale, sorted by rank). Flat = high entropy. Baselines drop steeply; GMM-JEPA stays flat.

Architectural choices are shared across all models including baselines; GMM anchoring + JEPA loss versus original WavLM loss objective is the only difference between GMM-JEPA and WavLM-style. See Appendix A for full specifications.

4 Experiments

Setup. Pre-trained on approximately 50,000 hours of speech from LibriLight large subset and English Granary [26]. To assess whether GMM anchoring generalizes across architectures, two encoder variants are evaluated: a Conformer-based encoder (GMM-JEPA) and a transformer-based encoder (GMM-JEPA-T). The transformer variant uses 10 standard transformer layers [31] with a 7-layer CNN frontend, enabling comparison across architectures. Both share identical GMM supervision and training procedures (Table 10). Baselines include Pure JEPA ($\lambda = 0$) and a WavLM-style baseline that uses our architecture with k-means clustering on log-mel features. This provides a controlled comparison that isolates the effect of GMM soft anchoring; direct comparison to published WavLM results would be confounded by differences in model size, training data, and compute.

Algorithm 1 GMM-Anchored JEPA Training

```

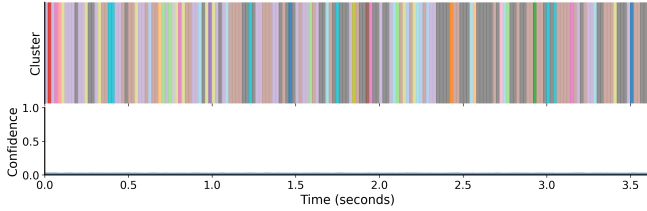
1: Phase 1: Fit GMM on log-mel features
2: Phase 2:
3: Init:  $f_\phi, f_{\phi'} \leftarrow f_\phi, h_\psi$ , cluster head,  $\mathbf{t}_{\text{mask}}$ 
4: for each minibatch  $\{\mathbf{x}\}$  do
5:    $\mathbf{x}_{\text{aug}}, \mathbf{x}_{\text{clean}} \leftarrow \text{Augment}(\mathbf{x})$ 
6:    $\mathbf{z}_{\text{online}} \leftarrow f_\phi(\mathbf{x}_{\text{aug}})$ 
7:    $\mathbf{z}_{\text{target}} \leftarrow f_{\phi'}(\mathbf{x}_{\text{clean}})$  {No grad}
8:    $q_{\text{gmm}} \leftarrow \text{GMM.posterior}(\text{LogMel}(\mathbf{x}_{\text{clean}}))$ 
9:    $m \leftarrow \text{SampleBlockMask}()$ 
10:   $\tilde{\mathbf{z}} \leftarrow m \odot \mathbf{z}_{\text{online}} + (1 - m) \odot \mathbf{t}_{\text{mask}}$ 
11:   $\mathbf{z}_{\text{pred}} \leftarrow h_\psi(\tilde{\mathbf{z}})$ 
12:   $p_{\text{cluster}} \leftarrow \text{softmax}(\text{ClusterHead}(\mathbf{z}_{\text{online}}))$ 
13:   $\mathcal{L}_{\text{JEPA}} \leftarrow \text{MSE}(\mathbf{z}_{\text{pred}}[\mathcal{M}], \mathbf{z}_{\text{target}}[\mathcal{M}])$ 
14:   $\mathcal{L}_{\text{cluster}} \leftarrow \text{KL}(q_{\text{gmm}}[\mathcal{M}] \parallel p_{\text{cluster}}[\mathcal{M}])$ 
15:   $\lambda \leftarrow \lambda_{\text{start}} + (\lambda_{\text{end}} - \lambda_{\text{start}}) \cdot t / T_{\text{max}}$ 
16:   $\mathcal{L} \leftarrow \mathcal{L}_{\text{JEPA}} + \lambda \cdot \mathcal{L}_{\text{cluster}}$ 
17:  Update  $\phi, \psi$  via  $\nabla \mathcal{L}$ 
18:   $\phi' \leftarrow \tau \phi' + (1 - \tau) \phi$  {EMA update}
19: end for

```

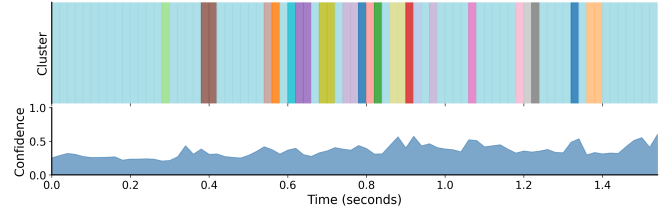
Evaluation. All downstream tasks train on frozen encoder representations. For ASR, a 2-layer BiLSTM with CTC loss [14] is trained on LibriSpeech train-clean-100 [27] with SpecAugment [28], using greedy decoding without a language model. For emotion recognition, a linear classifier is trained on mean-pooled representations using IEMOCAP [6] with 5-fold cross-validation over four emotions (angry, happy, sad, neutral). For slot filling, a sequence model is trained on SNIPS [11] with speaker-disjoint splits.

Results. Table 1 shows ASR performance. GMM-JEPA-T achieves 28.68% WER compared to 33.22% for WavLM-style. Pure JEPA produces 100% WER, confirming complete representation collapse [19, 29, 25] without acoustic grounding.

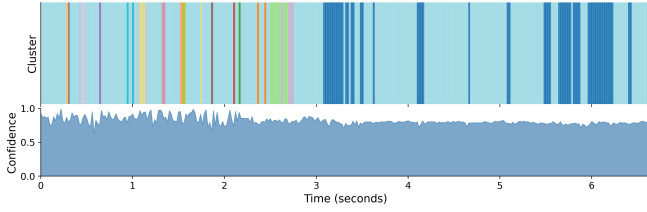
Table 2 shows slot filling results. GMM-JEPA achieves



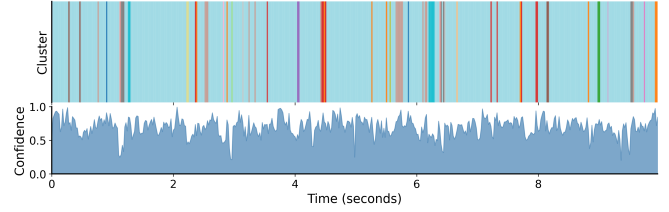
(a) Pure JEPA



(b) WavLM-style



(c) GMM-JEPA-T



(d) GMM-JEPA

Figure 4: **GMM-JEPA variants maintain stable, high-confidence clusters over time.** Top: cluster ID per frame. Bottom: confidence (1 – normalized entropy). (a) Pure JEPA flickers rapidly with near-zero confidence, indicating degenerate representations. (b) WavLM-style shows moderate confidence (0.4–0.6) with frequent cluster switching. (c) GMM-JEPA-T maintains high confidence (0.7–0.9) with moderate cluster and sparse transitions. (d) GMM-JEPA also shows moderate clusters with temporally coherent spans and moderate-to-high confidence (0.5–0.8).

Table 1: **GMM-JEPA reduces WER by 14% relative.** ASR on LibriSpeech dev-clean. Pure JEPA collapses (100% WER).

MODEL	WER (%) ↓	CER (%) ↓	Δ WER
PURE JEPA	100.00	93.11	–
WAVLM-STYLE	33.22	11.28	baseline
GMM-JEPA	29.18	9.62	–12.2%
GMM-JEPA-T	28.68	9.44	–13.7%

Table 2: **GMM-JEPA outperforms WavLM-style by 5.6% absolute.** Slot filling on SNIPS.

MODEL	TYPE F1 ↑	EDIT F1 ↑	Δ TYPE
PURE JEPA	5.0	2.2	–
WAVLM-STYLE	59.1	33.7	baseline
GMM-JEPA-T	59.2	32.8	+0.1
GMM-JEPA	64.7	36.0	+5.6

the highest Slot Type F1 (64.7%), outperforming WavLM-style by 5.6% absolute.

Table 3 shows emotion recognition results. GMM-JEPA-T and GMM-JEPA achieve 67.76% and 67.30% average accuracy respectively versus 65.46% for WavLM-style, with consistent improvement across all folds.

Table 3: **GMM-JEPA improves emotion recognition by 2% absolute.** SER accuracy (%) consistent across IEMOCAP folds.

MODEL	F1	F2	F3	F4	F5	Avg	Δ
PURE JEPA	48.88	46.12	49.89	48.67	46.97	48.11	–
WAVLM-STYLE	64.83	64.19	65.30	67.11	65.85	65.46	base
GMM-JEPA	66.07	67.85	66.67	68.56	67.37	67.30	+1.8
GMM-JEPA-T	67.19	67.52	67.58	68.11	68.41	67.76	+2.3

5 Analysis

To understand *why* GMM anchoring helps, the learned representations are analyzed through clustering and visualization.

Evaluation Methodology. Frame-level representations are extracted from each encoder on 1,000 utterances (up to 10 seconds each). Cluster assignments are obtained directly from each model’s learned cluster prediction head ($K = 1024$ classes), and two metrics are computed:

Cluster entropy measures vocabulary utilization:

$$H = - \sum_{k=1}^K p_k \log p_k, \quad p_k = \frac{|\{t : c_t = k\}|}{T_{\text{total}}}, \quad (7)$$

normalized by $\log K$ to yield a percentage. High entropy indicates all clusters are actively used; low entropy suggests collapse to few dominant clusters.

Adjacent consistency measures temporal smoothness:

$$\text{Consistency} = \frac{1}{T-1} \sum_{t=1}^{T-1} \mathbf{1}[c_t = c_{t+1}]. \quad (8)$$

Table 4: **GMM-JEPA achieves 98% entropy vs. 31% for WavLM-style.** Cluster analysis metrics with $K = 1024$.

MODEL	ENTROPY \uparrow	USED \uparrow	ADJ. CONS.
PURE JEPA	45%	516	0.205
WavLM-STYLE	31%	978	0.750
GMM-JEPA	85%	1007	0.395
GMM-JEPA-T	98%	1013	0.299

Since phonemes typically span 50–200ms [20] while frames are 20ms, acoustically meaningful clusters should persist across adjacent frames rather than flickering rapidly.

For visualization, 10,000 randomly sampled frames are projected to 2D via UMAP [24] and colored by their predicted cluster assignment (top 10 clusters highlighted).

Results. Table 4 summarizes the quantitative findings.

The results reveal clear differences between methods. Pure JEPA achieves only 45% entropy using 516/1024 clusters, indicating severe representation collapse [19] where half the cluster vocabulary is unused. WavLM-style performs even worse in terms of entropy (31%) despite using more clusters (978/1024), indicating extreme imbalance where a few clusters dominate while most are rarely assigned, a phenomenon observed in other self-supervised methods [7].

In contrast, both GMM-anchored variants achieve substantially higher entropy. GMM-JEPA reaches 85% entropy with 1007/1024 clusters used, while GMM-JEPA-T achieves the best result at 98% entropy with 1013/1024 clusters. This demonstrates that GMM anchoring effectively prevents the representation collapse observed in both Pure JEPA and WavLM-style training.

Qualitative Analysis. Figure 2 visualizes the representation space via UMAP projection. Pure JEPA collapses to a small, dense region with limited cluster diversity. WavLM-style spreads across a larger area but exhibits diffuse, overlapping cluster assignments with no clear separation. GMM-JEPA-T and GMM-JEPA both form localized, well-separated cluster regions distributed across the embedding space, demonstrating cleaner partitioning of the latent space.

Figure 3 confirms the entropy findings through cluster utilization distributions. Pure JEPA shows a steep dropoff after approximately 270 clusters, with the remaining clusters receiving near-zero assignments. WavLM-style also exhibits a steeper dropoff despite broader cluster usage, explaining its low entropy. Both GMM-anchored variants maintain substantially flatter distributions, with GMM-JEPA-T showing the most uniform utilization across all 1024 clusters. Figure 4 examines cluster assignment behavior over time. Pure JEPA shows near-zero prediction

Table 5: **All anchored models saturate on speaker/gender; Pure JEPA fails.** Linear probe accuracy (%) on paralinguistic categories.

MODEL	SPEAKER \uparrow	GENDER \uparrow
PURE JEPA	18.7 ± 1.8	69.2 ± 1.5
WavLM-STYLE	99.6 ± 0.3	99.4 ± 0.2
GMM-JEPA-T	99.7 ± 0.2	99.7 ± 0.2
GMM-JEPA	99.8 ± 0.2	99.6 ± 0.3

Table 6: **GMM-JEPA improves phoneme classification by +5.4% (linear) and +6.7% (MLP).** Phoneme probe accuracy (%).

MODEL	LINEAR \uparrow	MLP \uparrow
PURE JEPA	7.4 ± 0.0	9.0 ± 0.1
WavLM-STYLE	47.6 ± 0.2	57.5 ± 0.2
GMM-JEPA-T	51.4 ± 0.1	59.4 ± 0.4
GMM-JEPA	53.0 ± 0.1	64.2 ± 0.2

confidence with rapid cluster flickering, indicating degenerate representations. WavLM-style collapses to a smaller set of dominant clusters with moderate confidence, explaining its low entropy despite using many clusters. In contrast, both GMM-JEPA variants maintain higher confidence than their WavLM and Pure JEPA counterparts with temporally coherent cluster spans, demonstrating that GMM anchoring produces stable, meaningful cluster assignments.

5.1 Embedding Quality Analysis

Cluster Quality Analysis. To assess representational similarity across models, embeddings are clustered via K-means and compared using Normalized Mutual Information (NMI). NMI measures the agreement between two clusterings, defined as:

$$NMI(U, V) = \frac{2 \cdot I(U; V)}{H(U) + H(V)}, \quad (9)$$

where $I(U; V)$ is the mutual information between clusterings U and V , and $H(\cdot)$ denotes entropy. NMI ranges from 0 (independent) to 1 (identical).

Linear Probe Evaluation. Linear probes are trained to assess how well frozen embeddings classify both high-level paralinguistic categories (Speaker ID, Gender) and low-level linguistic units (phonemes). All models are trained for the same number of speech hours to ensure fair comparison. Results are shown in Table 5 and Table 6.

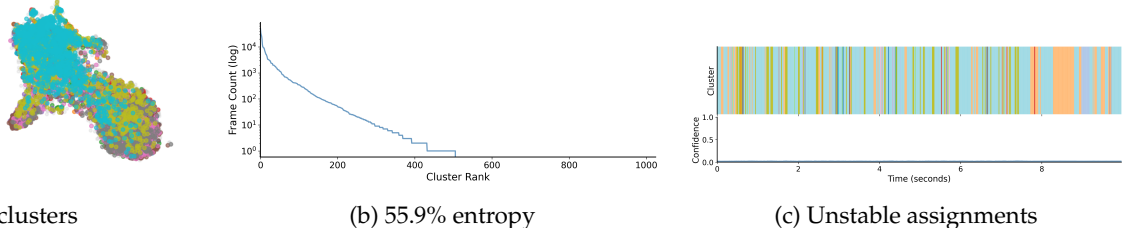


Figure 5: **Removing residual GMM supervision ($\lambda_{\text{end}} = 0$) causes collapse.** Without ongoing anchoring, representations deteriorate. (a) UMAP shows overlapping clusters. (b) Only 506/1024 clusters used. (c) Confidence drops, flickering increases.

Table 7: **Pure JEPA shares no structure with other models (NMI<0.11).** NMI between embedding clusters.

	PURE	WavLM	GMM	GMM-T
PURE JEPA	1.00	0.08	0.11	0.06
WavLM-STYLE	0.08	1.00	0.47	0.57
GMM-JEPA	0.11	0.47	1.00	0.47
GMM-JEPA-T	0.06	0.57	0.47	1.00

Pure JEPA fails catastrophically across all metrics (18.7% speaker, 7.4% phoneme), confirming that acoustic grounding is essential for learning meaningful representations. GMM-JEPA consistently matches or outperforms WavLM-style, with notable improvements in phoneme classification (+5.4% linear, +6.7% MLP). GMM-JEPA-T achieves comparable performance, demonstrating that the benefits of GMM anchoring transfer across architectures. Table 7 shows NMI between embedding clusters.

Pure JEPA shows minimal similarity to all other models (NMI<0.11), consistent with the representation collapse observed in Section 5. The three successful models exhibit moderate mutual similarity (NMI=0.47–0.57), indicating they capture related but distinct acoustic structure. GMM-JEPA and GMM-JEPA-T show medium similarity (NMI=0.47), suggesting that architecture influences representation geometry independently of training objective.

Cluster-Label Alignment. Finally, the alignment between unsupervised clusters and supervised labels is measured via NMI (Table 8).

GMM-JEPA achieves the highest alignment for Speaker (0.48) and Gender (0.15), substantially outperforming WavLM-style on paralinguistic categories. GMM-JEPA-T achieves the highest phoneme alignment (0.24), sug-

Table 8: **GMM-JEPA captures speaker/gender; GMM-JEPA-T captures phonemes.** Cluster-label alignment (NMI).

MODEL	PHONEME \uparrow	SPEAKER \uparrow	GENDER \uparrow
PURE JEPA	0.03	0.14	0.02
WavLM-STYLE	0.20	0.27	0.10
GMM-JEPA	0.19	0.48	0.15
GMM-JEPA-T	0.24	0.22	0.10

gesting the transformer architecture better preserves fine-grained linguistic structure. The Conformer architecture appears to emphasize paralinguistic structure while the Transformer preserves finer phonetic detail; this architectural difference is orthogonal to GMM anchoring, which improves both variants over their respective baselines. These results indicate that GMM anchoring encourages representations that capture speaker-level information more effectively, which may explain the improved emotion recognition performance observed in Table 3.

5.2 Ablation: GMM Anchoring

A natural question is whether GMM supervision can be fully removed after the initial grounding phase. To investigate, a GMM-JEPA model is trained with λ decaying to zero rather than to 0.01 (i.e., disabling GMM loss in late training).

As shown in Table 9, removing residual GMM supervision causes severe deterioration across both representation quality and downstream performance. Entropy drops from 84.7% to 57.7%, and cluster utilization falls from 1011 to 506 clusters, approximately the same as Pure JEPA’s collapsed state (45% entropy, 516 clusters). Critically, this

Table 9: **Anchoring is essential: $\lambda_{\text{end}} = 0$ degrades WER to 40.9%.** Effect of removing GMM supervision after decay.

λ_{END}	ENT. \uparrow	USED \uparrow	WER \downarrow	SER \uparrow	SF-T \uparrow	SF-E \uparrow
0.00	57.7	530	40.9	63.8	62.3	34.2
0.01	84.7	1011	29.2	67.3	64.7	36.0

degradation translates directly to downstream tasks: WER increases from 29.18% to 40.95%, SER accuracy drops from 67.30% to 63.79%, and slot filling performance decreases across both Type F1 (64.7% to 62.3%) and Edit F1 (36.0% to 34.2%).

Figure 5 confirms this degradation visually. The UMAP projection (Figure 5a) shows that without residual anchoring, clusters become diffuse and overlapping, losing the well-separated structure observed in GMM-JEPA. The cluster distribution (Figure 5b) exhibits a steep dropoff, with nearly half the clusters receiving negligible assignments. The confidence plot (Figure 5c) shows reduced confidence with increased cluster flickering compared to the stable, high-confidence assignments of GMM-JEPA ($\lambda_{\text{end}} = 0.01$).

These results demonstrate that GMM anchoring provides ongoing regularization, not merely initialization. Even minimal supervision ($\lambda = 0.01$) prevents the representational drift that occurs when the JEPA objective dominates unconstrained, and this regularization is essential for maintaining downstream task performance.

6 Discussion

Our results demonstrate that frozen GMM supervision addresses a core challenge in JEPA-based speech SSL: without external grounding, the EMA teacher provides no spectral information, allowing representations to collapse to acoustically meaningless states. The GMM provides this grounding through two mechanisms. First, early training ($\lambda = 1.0$) forces the encoder to predict acoustic cluster posteriors, establishing phonetically meaningful structure before the JEPA objective can cause collapse. Second, residual supervision ($\lambda = 0.01$) maintains this structure throughout training, as our ablation shows that removing the anchor causes representations to deteriorate even after initial grounding.

We hypothesize that the soft assignment property of GMMs provides an advantage over hard k-means clustering. At acoustic boundaries where frames are ambiguous between phonetic categories, GMM posteriors preserve this uncertainty rather than forcing arbitrary hard decisions. This may explain why GMM-JEPA achieves higher cluster entropy (85–98%) compared to WavLM-style (31%), which uses hard assignments that concentrate probability mass on dominant clusters. Validating this hypothesis by comparing soft GMM posteriors against hard GMM

assignments remains future work.

Limitations & Future Work. Our models are trained on 50k hours in a single pass, while HuBERT and WavLM use iterative re-clustering with multiple passes, effectively multiplying training compute. We focus on demonstrating that frozen GMM supervision provides effective acoustic grounding for JEPA rather than achieving state-of-the-art absolute performance; we do not compare against published HuBERT/WavLM checkpoints due to confounds in architecture and training data. We do not ablate soft versus hard GMM assignments, leaving validation of the soft assignment hypothesis for future work. The optimal decay schedule and residual weight ($\lambda_{\text{end}} = 0.01$) were selected based on preliminary experiments but not extensively tuned. Additionally, we evaluate on English speech only.

Promising directions include: (1) allowing the GMM to adapt during training rather than remaining frozen, potentially capturing evolving acoustic structure; (2) exploring alternative anchors such as neural density estimators; (3) extending to multilingual settings where iterative re-clustering becomes computationally prohibitive; and (4) investigating whether GMM anchoring benefits other JEPA domains beyond speech.

7 Conclusion

We introduced GMM-Anchored JEPA, a framework that grounds self-supervised speech representations with frozen Gaussian Mixture Model supervision. By fitting a GMM once on log-mel spectrograms and using its soft posteriors as auxiliary targets with a decaying weight schedule, we eliminate the need for iterative re-clustering while preserving uncertainty at acoustic boundaries. Experiments on 50k hours of speech show that GMM anchoring improves ASR, emotion recognition, and slot filling compared to WavLM-style baselines with matched compute, while achieving substantially higher cluster entropy (98% vs. 31%). Ablation studies confirm that residual GMM supervision provides ongoing regularization essential for preventing representation collapse. Our results suggest that simple, frozen acoustic anchors can effectively stabilize JEPA training for speech, opening new directions for efficient self-supervised speech representation learning.

Impact Statement

This work advances self-supervised speech representation learning, with applications in ASR, emotion recognition, and spoken language understanding. Improved representations could benefit accessibility tools and low-resource languages. However, these representations could potentially be misused for surveillance or voice profiling. We encourage responsible deployment with appropriate consent and privacy protections.

References

- [1] Mahmoud Assran, Quentin Duval, Ishan Misra, Piotr Bojanowski, Pascal Vincent, Michael Rabbat, Yann LeCun, and Nicolas Ballas. Self-supervised learning from images with a joint-embedding predictive architecture. In *CVPR*, 2023.
- [2] Alexei Baevski, Wei-Ning Hsu, Qiantong Xu, Arun Babu, Jiatao Gu, and Michael Auli. data2vec: A general framework for self-supervised learning in speech, vision and language. In *ICML*, 2022.
- [3] Alexei Baevski, Yuhao Zhou, Abdelrahman Mohamed, and Michael Auli. wav2vec 2.0: A framework for self-supervised learning of speech representations. In *NeurIPS*, 2020.
- [4] James C Bezdek. *Pattern Recognition with Fuzzy Objective Function Algorithms*. Springer, 1981.
- [5] Christopher M Bishop. *Pattern Recognition and Machine Learning*. Springer, 2006.
- [6] Carlos Busso, Murtaza Bulut, Chi-Chun Lee, Abe Kazemzadeh, Emily Mower, Samuel Kim, Jeanette N Chang, Sungbok Lee, and Shrikanth S Narayanan. Iemocap: Interactive emotional dyadic motion capture database. *Language Resources and Evaluation*, 42(4):335–359, 2008.
- [7] Mathilde Caron, Ishan Misra, Julien Mairal, Priya Goyal, Piotr Bojanowski, and Armand Joulin. Unsupervised learning of visual features by contrasting cluster assignments, 2021.
- [8] Mathilde Caron, Hugo Touvron, Ishan Misra, Hervé Jégou, Julien Mairal, Piotr Bojanowski, and Armand Joulin. Emerging properties in self-supervised vision transformers. In *ICCV*, 2021.
- [9] Sanyuan Chen, Chengyi Wang, Zhengyang Chen, Yu Wu, Shujie Liu, Zhuo Chen, Jinyu Li, Naoyuki Kanda, Takuya Yoshioka, Xiong Xiao, et al. Wavlm: Large-scale self-supervised pre-training for full stack speech processing. In *IEEE JSTSP*, 2022.
- [10] Chung-Cheng Chiu, James Qin, Yu Zhang, Jiahui Yu, and Yonghui Wu. Self-supervised learning with random-projection quantizer for speech recognition. In *ICML*, 2022.
- [11] Alice Coucke, Alaa Saade, Adrien Ball, Théodore Bluche, Alexandre Caulier, David Leroy, Clément Doumouro, Thibault Gisselbrecht, Francesco Caltagirone, Thibaut Lavril, Maël Primet, and Joseph Dureau. Snips voice platform: an embedded spoken language understanding system for private-by-design voice interfaces, 2018.
- [12] Yann N Dauphin, Angela Fan, Michael Auli, and David Grangier. Language modeling with gated convolutional networks. In *ICML*, 2017.
- [13] Andrew Drozdov, Ravid Shwartz-Ziv, and Yann LeCun. Video joint embedding predictive architecture with variance-covariance regularization. *arXiv preprint arXiv:2412.10925*, 2024.
- [14] Alex Graves, Santiago Fernández, Faustino Gomez, and Jürgen Schmidhuber. Connectionist temporal classification: Labelling unsegmented sequence data with recurrent neural networks. In *ICML*, 2006.
- [15] Jean-Bastien Grill, Florian Strub, Florent Altché, Corentin Tallec, Pierre Richemond, Elena Buchatskaya, Carl Doersch, Bernardo Avila Pires, Zhaohan Guo, Mohammad Gheshlaghi Azar, et al. Bootstrap your own latent: A new approach to self-supervised learning. In *NeurIPS*, 2020.
- [16] Wei-Ning Hsu, Benjamin Bolte, Yao-Hung Hubert Tsai, Kushal Lakhotia, Ruslan Salakhutdinov, and Abdelrahman Mohamed. Hubert: Self-supervised speech representation learning by masked prediction of hidden units. In *IEEE/ACM TASLP*, 2021.
- [17] Georgios Ioannides, Aman Chadha, and Aaron Elkins. Density adaptive attention is all you need: Robust parameter-efficient fine-tuning across multiple modalities. *arXiv preprint arXiv:2401.11143*, 2024.
- [18] Georgios Ioannides, Adrian Kieback, Aman Chadha, and Aaron Elkins. Density adaptive attention-based speech network: Enhancing feature understanding for mental health disorders. *arXiv preprint arXiv:2409.00391*, 2024.
- [19] Li Jing, Pascal Vincent, Yann LeCun, and Yuandong Tian. Understanding dimensional collapse in contrastive self-supervised learning, 2022.
- [20] Peter Ladefoged and Keith Johnson. *A Course in Phonetics*. Cengage Learning, 7th edition, 2014.
- [21] Yann LeCun. A path towards autonomous machine intelligence. *OpenReview*, 2022.
- [22] Ilya Loshchilov and Frank Hutter. Decoupled weight decay regularization. *ICLR*, 2019.
- [23] James MacQueen. Some methods for classification and analysis of multivariate observations. In *Proceedings of the Fifth Berkeley Symposium on Mathematical Statistics and Probability*, 1967.
- [24] Leland McInnes, John Healy, and James Melville. Umap: Uniform manifold approximation and projection for dimension reduction, 2020.
- [25] Shentong Mo and Shida Tong. Connecting joint-embedding predictive architecture with contrastive self-supervised learning. In *NeurIPS*, 2024.

- [26] Koluguri Nithin Rao et al. Granary: A large-scale multilingual speech corpus. *arXiv preprint*, 2025.
- [27] Vassil Panayotov, Guoguo Chen, Daniel Povey, and Sanjeev Khudanpur. Librispeech: An asr corpus based on public domain audio books. In *ICASSP*, 2015.
- [28] Daniel S. Park, William Chan, Yu Zhang, Chung-Cheng Chiu, Barret Zoph, Ekin D. Cubuk, and Quoc V. Le. Specaugment: A simple data augmentation method for automatic speech recognition. In *Interspeech 2019, interspeech_2019*, page 2613–2617. ISCA, September 2019.
- [29] Emanuele Sansone, Thibault Lebailly, and Tinne Tuytelaars. Collapse-proof non-contrastive self-supervised learning. *arXiv preprint arXiv:2410.04959*, 2024.
- [30] Aaron van den Oord, Yazhe Li, and Oriol Vinyals. Representation learning with contrastive predictive coding. In *arXiv preprint arXiv:1807.03748*, 2018.
- [31] Ashish Vaswani, Noam Shazeer, Niki Parmar, Jakob Uszkoreit, Llion Jones, Aidan N Gomez, Łukasz Kaiser, and Illia Polosukhin. Attention is all you need. In *NeurIPS*, 2017.
- [32] Liu Ziyin, Tilman Hartwig, and Masahito Ueda. Neural networks fail to learn periodic functions and how to fix it. In *NeurIPS*, 2020.

A Architecture Details

A.1 Encoder Backbone

The encoder consists of strided convolutional blocks followed by a Conformer stack.

Input Convolution. A 7-kernel convolution maps raw waveform to initial features:

$$h_0 = \text{Conv1d}_{1 \rightarrow C_0}^{k=7, p=3}(\mathbf{x}). \quad (10)$$

Strided Encoder Blocks. Each block i with stride s_i applies:

1. Strided convolution with kernel $2s_i$, stride s_i , padding $s_i/2$
2. Snake-Beta activation (see below)
3. Residual blocks with dilated convolutions (dilation pattern $[1, 3, 5]$ per block)
4. Density Adaptive Attention block

Channel progression $[32, 64, 128, 256]$ with strides $[8, 8, 5]$ yields total stride 320.

Conformer Stack. $N_{\text{conf}} = 4$ Conformer layers with:

- Half-step feed-forward modules (expansion factor 4)
- Multi-head self-attention (32 heads) with gated relative position bias
- Depthwise separable convolution module with GLU activation [12] (kernel size 31)

Each Conformer block applies:

$$x = x + \frac{1}{2} \text{FFN}_1(x), \quad (11)$$

$$x = x + \text{MHSA}(x), \quad (12)$$

$$x = x + \text{ConvModule}(x), \quad (13)$$

$$x = x + \frac{1}{2} \text{FFN}_2(x). \quad (14)$$

A.2 Snake-Beta Activation

$$\text{Snake}_\alpha(x) = x + \frac{\sin^2(\alpha x)}{\alpha}, \quad \alpha = \text{softplus}(a) + 0.01, \quad (15)$$

where $a \in \mathbb{R}^{1 \times C \times 1}$ is a learnable parameter per channel.

A.3 Gated Relative Position Bias

Position Embedding. Relative positions are mapped to buckets via logarithmic bucketing:

$$\text{bucket}(i - j) = \begin{cases} |i - j| & \text{if } |i - j| < \frac{B}{4} \\ \frac{B}{4} + \frac{B}{4} \cdot \frac{\log(|i - j| / \frac{B}{4})}{\log(D_{\text{max}} / \frac{B}{4})} & \text{otherwise} \end{cases} \quad (16)$$

where $B = 320$ buckets and $D_{\text{max}} = 800$ maximum distance.

Gating Mechanism. Per-position gates computed from queries $\mathbf{q} \in \mathbb{R}^{B \times H \times T \times d}$:

$$g_{\text{update}} = \sigma(\mathbf{q} \cdot \mathbf{u}), \quad (17)$$

$$g_{\text{reset}} = \sigma(\mathbf{q} \cdot \mathbf{w}), \quad (18)$$

where $\mathbf{u}, \mathbf{w} \in \mathbb{R}^{H \times d}$ are learnable vectors.

Gated Bias. Final position bias combines learned embeddings with gating:

$$\tilde{r}_{i-j} = s \cdot g_{\text{reset},i} \cdot d_{i-j}, \quad (19)$$

$$r_{i-j} = d_{i-j} + g_{\text{update},i} \cdot d_{i-j} + (1 - g_{\text{update},i}) \cdot \tilde{r}_{i-j}, \quad (20)$$

where d_{i-j} is the learned embedding and s is a learnable scale.

A.4 Layer Aggregation

Given Conformer layer outputs $\{z^{(l)}\}_{l=0}^L$:

$$\mathbf{Q} = W_Q \cdot \text{pool}(z^{(L)}), \quad (21)$$

$$\mathbf{K} = W_K \cdot \text{stack}(\text{pool}(z^{(l)})), \quad (22)$$

$$\mathbf{V} = W_V \cdot \text{stack}(\text{pool}(z^{(l)})), \quad (23)$$

$$\text{weights} = \text{softmax}(\mathbf{Q}\mathbf{K}^\top / \sqrt{d}), \quad (24)$$

$$z_{\text{agg}} = \sum_l \text{weights}_l \cdot z^{(l)}, \quad (25)$$

where pooling is over the time dimension and attention operates over layers.

A.5 Density Adaptive Attention (DAAM)

DAAM [17, 18] computes attention weights using a product of Gaussian kernels over normalized activations. For input $x \in \mathbb{R}^{B \times C \times T}$:

Normalization. Input is standardized along the attention axis:

$$\bar{x} = \frac{x - \mu_x}{\sigma_x + \epsilon}. \quad (26)$$

Gaussian Mixture Weights. For N_g Gaussians with learnable offsets δ_i and scales c_i :

$$\log w_i = -\frac{(\bar{x} - \delta_i)^2}{2c_i^2} - \frac{1}{2} \log(2\pi c_i^2), \quad (27)$$

$$\log w = \sum_{i=1}^{N_g} \log w_i. \quad (28)$$

Output. Attention is applied with residual connection:

$$\text{out} = x \odot \text{softmax}(\log w) + x. \quad (29)$$

The input is split along the channel dimension into H heads, each processed by an independent DAAM module, then concatenated.

A.6 Cluster Prediction Head

A multi-layer MLP with residual connections maps encoder outputs to K cluster logits:

$$h_0 = \text{GELU}(\text{LayerNorm}(\text{Linear}_{C \rightarrow H}(z))), \quad (30)$$

$$h_l = h_{l-1} + \text{Block}_l(h_{l-1}), \quad l = 1, \dots, L_{\text{head}}, \quad (31)$$

$$\text{logits} = \text{Linear}_{H \rightarrow K}(\text{LayerNorm}(h_{L_{\text{head}}})), \quad (32)$$

where each block contains $\text{LayerNorm} \rightarrow \text{Linear} \rightarrow \text{GELU} \rightarrow \text{Dropout} \rightarrow \text{Linear} \rightarrow \text{Dropout}$ with residual.

A.7 Predictor Architecture

The predictor consists of: (1) Conv1d projection: $C \rightarrow C$, (2) GELU activation, (3) Single Conformer block (shared relative position bias with encoder), and (4) Conv1d output projection: $C \rightarrow C$.

A.8 Target Encoder and EMA Update

The target encoder has identical architecture but parameters are updated via EMA after each gradient step:

$$\phi' \leftarrow \tau\phi' + (1 - \tau)\phi, \quad \tau = 0.996. \quad (33)$$

B Training Hyperparameters

Table 10: Training hyperparameters.

	CONFORMER	TRANSFORMER
<i>Encoder Architecture</i>		
PARAMETERS	31.1M	41.3M
CNN LAYERS	3	7
CHANNELS	[32,64,128,256]	[256] \times 7
STRIDES	[8,8,5]	[5,2,2,2,2,2,2]
LATENT DIM	512	512
ENCODER LAYERS	4	10
ATTENTION HEADS	32	8
FFN MULT / DIM	4 \times 512	2048
CONV KERNEL	31	-
<i>GMM Fitting</i>		
COMPONENTS K		1024
MEL BINS		80
INITIALIZATION		K-MEANS++
OPTIMIZATION		MINI-BATCH SGD
LEARNING RATE		$10^{-2} \rightarrow 10^{-4}$ (COSINE)
TRAINING FRAMES		9.6B
<i>K-Means Fitting (WavLM-style baseline)</i>		
COMPONENTS K		1024
FEATURE TYPE		LOG-MEL (80 BINS)
INITIALIZATION		K-MEANS++
UPDATE METHOD		LLOYD'S ALGORITHM
LLOYD ITERATIONS		20
TRAINING FRAMES		9.6B
<i>Training</i>		
OPTIMIZER		ADAMW [22]
LEARNING RATE		$10^{-5} \rightarrow 10^{-4} \rightarrow 10^{-5}$
LR SCHEDULE		10% LINEAR WARMUP / DECAY
WEIGHT DECAY		10^{-3}
MICRO BATCH SIZE	96 (CONFORMER)	192 (TRANSF.)
GRADIENT CLIPPING		1.0
GPUs		8 \times B200
EMA τ		0.996
λ DECAY		$1.0 \rightarrow 0.01$
MASK RATIO		[0.4, 0.65]
SPAN LENGTH		[10, 25] FRAMES
<i>Augmentation</i>		
NOISE SNR		[-5, 20] dB
MIX RATIO		[-5, 5] dB
NOISE / MIX PROB.		0.25 EACH

C GMM Details

C.1 Posterior Computation

The posterior with diagonal covariance is computed as:

$$q_k(\mathbf{m}) = \text{softmax}_k \left(\log \pi_k - \frac{D}{2} \log(2\pi) - \frac{1}{2} \sum_{d=1}^D \left[\log \sigma_{k,d}^2 + \frac{(m_d - \mu_{k,d})^2}{\sigma_{k,d}^2} \right] \right). \quad (34)$$

C.2 Chunked Soft Assignment

To prevent out-of-memory errors with large K and batch sizes, soft assignment is computed in chunks:

Algorithm 2 Chunked Soft Assignment

```

1: Input: Features  $X \in \mathbb{R}^{N \times D}$ , GMM parameters, chunk sizes
2: Output: Posteriors  $Q \in \mathbb{R}^{N \times K}$ 
3: for  $n = 0$  to  $N$  step batch_size do
4:   for  $k = 0$  to  $K$  step chunk_k do
5:      $\Delta \leftarrow X[n : n'] - \mu[k : k'] \{[B, K', D]\}$ 
6:     mahal  $\leftarrow \sum_d \Delta_d^2 / \sigma_{k,d}^2$ 
7:      $\log p_{n,k} \leftarrow -\frac{D}{2} \log(2\pi) - \frac{1}{2} \sum_d \log \sigma_{k,d}^2 - \frac{1}{2} \text{mahal}$ 
8:   end for
9:    $Q[n : n'] \leftarrow \text{softmax}(\log \pi + \log p)$ 
10: end for

```

D Augmentation Details

D.1 Energy-Based SNR Mixing

Given clean signal x and noise n , mixing at target SNR:

$$E_x = \frac{1}{|x|} \sum_i x_i^2, \quad E_n = \frac{1}{|n|} \sum_i n_i^2, \quad (35)$$

$$\alpha = \sqrt{\frac{E_x}{10^{\text{SNR}/10} \cdot E_n}}, \quad (36)$$

$$x_{\text{aug}} = x + \alpha \cdot n, \quad (37)$$

where SNR is sampled from $[-5, 20]$ dB with probability 0.25.

D.2 Utterance Mixing

A segment from another utterance is mixed with the primary:

1. Sample mix length: $L_{\text{mix}} \leftarrow \text{randint}(1, |x_1| \cdot 0.5)$
2. Sample start positions t_1, t_2 in primary and secondary
3. Extract regions: $r_1 \leftarrow x_1[t_1 : t_1 + L], r_2 \leftarrow x_2[t_2 : t_2 + L]$
4. Compute energies E_1, E_2
5. Sample energy ratio: $\rho \sim \text{Uniform}(-5, 5)$ dB
6. Compute scale: $\beta \leftarrow \sqrt{E_1 \cdot 10^{\rho/10} / E_2}$
7. Mix: $x_1[t_1 : t_1 + L] \leftarrow r_1 + \beta \cdot r_2$

Mixing probability is 0.25 with max 50% overlap.

Table 11: SER accuracy (%) per fold for $\lambda_{\text{end}} = 0$ ablation.

λ_{END}	F1	F2	F3	F4	F5	AVG
0.00	63.48	63.41	63.70	63.22	65.15	63.79
0.01	66.07	67.85	66.67	68.56	67.37	67.30

D.3 Augmentor Buffer

The augmentor maintains a buffer of 64 recent utterances for noise/mixing sources, updated after each batch and stored on CPU.

E Visualization Details

UMAP Projection. Table 12 lists the hyperparameters used for UMAP projections in Figure 2.

Table 12: UMAP hyperparameters.

PARAMETER	VALUE
N_NEIGHBORS	15
MIN_DIST	0.1
METRIC	EUCLIDEAN
N_COMPONENTS	2
RANDOM_STATE	42
N_SAMPLES	10,000